perfluoroalkyl chains, guest **5**, solvents, and counter ions. Hence the *R* value of 24.6% is quite reasonable given the size and complexity of the compound.
17. This work was financially supported by a Grant-in-Aid for Scientific Research (S) no. 14103014, from the Ministry of Education, Culture, Sports, Science, and Technology of Japan. Supplementary crystallographic data for compound **2a** can be obtained free of charge (under CCDC 602076) by contacting the Cambridge Crystallographic Data Centre, 12, Union Road, Cambridge CB2 1EZ, UK; via their Web site (www.ccdc.cam.ac.uk/data_request/cif), by e-mail (data_request@ccdc.cam.ac.uk), or by fax (+44 1223 336033). We thank K. Yamaguchi and H. Masu for CHNS elemental analyses.

Supporting Online Material
www.sciencemag.org/cgi/content/full/313/5791/1273/DC1
Materials and Methods
Figs. S1 to S8

11 May 2006; accepted 20 July 2006
10.1126/science.1129830

Triple-Bond Reactivity of Diphosphorus Molecules

Nicholas A. Piro, Joshua S. Figueroa, Jessica T. McKellar, Christopher C. Cummins*

We report a mild method for generating the diphosphorus molecule or its synthetic equivalent in homogeneous solution; the P_2 allotrope of the element phosphorus is normally obtained only under extreme conditions (for example, from P_4 at 1100 kelvin). Diphosphorus is extruded from a niobium complex designed for this purpose and can be trapped efficiently by two equivalents of an organic diene to produce an organodiphosphorus compound. Diphosphorus stabilized by coordination to tungsten pentacarbonyl can be generated similarly at 25°C, and in this stabilized form it still efficiently consumes two organic diene molecules for every diphosphorus unit.

A dichotomy exists in the chemistry of the group 15 elements: The stable molecular form of nitrogen is triply bonded dinitrogen, whereas the stable molecular form of phosphorus is the tetrahedral P_4 molecule, white phosphorus (*1*). Only upon heating white phosphorus to more than 1100 K does the P_4 = 2 P_2 equilibrium become important (*2*–*4*). Underlying this dichotomy is the tendency of nitrogen to engage in multiple bonding, as compared with phosphorus, for which the π-bond components of multiple bonds are relatively high in energy and quite reactive (*5*, *6*). Thus, the triple bond in the atmospherically abundant dinitrogen molecule is one of the strongest known chemical bonds (its bond dissociation enthalpy, D_e, is 226 kcal/mol), whereas that in the diphosphorus molecule is only about half as strong (D_e = 117 kcal/mol) (*7*, *8*). P_2 is therefore known principally as an exotic gas-phase species of astrophysical interest (*9*), as a reactive component of plasmas generated in the high-temperature deposition of III/V semiconductor materials (*10*), and in the context of matrix-isolation experiments (*11*–*14*). The use of P_2 in chemical synthesis requires a means to generate it in solution and under mild conditions of temperature and pressure. Accordingly, we describe a mild method that uses niobium chemistry as a vehicle for the generation of diphosphorus (or a synthetic equivalent) in solution, where it may be trapped by suitable organic acceptors.

Organic azides, molecules of formula N=N=N–R, where R is a variable organic substituent, are known to react with transfer of their nitrene moiety (N–R) to a group 5 metal through observable or isolable intermediates, in which an intact RN_3 molecule is complexed (*15*–*17*). The final products in such a nitrene transfer reaction are the group 5 metal imido and N_2 gas (Fig. 1A). Diphosphorus-substituted analogs of organic azides, of formula P=P=N–R, would be a useful addition to the library of low-coordinate phosphorus compounds (*5*), and we wondered whether they would react analogously with group 5 metals to transfer nitrene while extruding the desired P_2 molecule (Fig. 1B).

To synthesize such a solution-phase P_2-generating molecular system, we created the phosphorus-phosphorus bond within the protective coordination sphere of a niobium complex. Recently, we have used the terminal phosphide anion $[P{\equiv}Nb(N[Np]Ar)_3]^{1-}$ (where Np is neopentyl and Ar is 3,5-$C_6H_3Me_2$) as its sodium salt to great advantage in assembling phosphorus-element bonds atop the protective $Nb(N[Np]Ar)_3$ platform (*18*, *19*), and the present work is a logical extension of that methodology.

The system (η^2-Mes*NPP)$Nb(N[Np]Ar)_3$ (where Mes* is 2,4,6-*t*-$Bu_3C_6H_2$), **1**, containing the diphosphorus-substituted organic azide ligand bound through its P_2 unit to the niobium trisanilide platform, has been obtained in 60% isolated yield as an orange-red solid after an NaCl-elimination reaction between Niecke's chloroiminophosphane ClP=NMes* (*20*) and our terminal phosphide anion sodium salt, $Na[P{\equiv}Nb(N[Np]Ar)_3]$ (*21*). Complex **1** has been characterized by single-crystal x-ray crystallography (Fig. 2A); the structure so obtained is notable for its short P=P and P=N interatomic distances [2.0171(±0.0009) and 1.556 (±0.002) Å (where the error is estimated standard deviation), respectively], which suggest multiple bonding between these atoms. Characterization data for **1** obtained by nuclear magnetic resonance (NMR) spectroscopy (^{31}P, ^{13}C, and ^{1}H) in benzene-d_6 solution are consistent with the observed solid-state structure of the complex, with the ^{31}P data [doublets with a one-bond P-P coupling constant $^{1}J_{PP}$ = 650 Hz at a chemical shift, δ, of 334 and 315 parts per million (ppm)] being most diagnostic for the system. Alternative isomeric formulations of **1** may be similar in energy to the solid-state structure of **1**, and we considered them in our computational studies.

Heating a solution of complex **1** in neat 1,3-cyclohexadiene (1,3-CHD), the latter serving both as solvent and as trap for the P_2 unit, to 65°C for 3 hours gave smooth and quantitative conversion to niobium imido **2** together with a single phosphorus-containing product. This product (**3** in Fig. 2A) is characterized by a singlet in the ^{31}P NMR spectrum at δ = −80 ppm. Formulation of **3** as the double Diels-Alder (*22*) adduct of P_2 with two equivalents of 1,3-CHD was confirmed by its isolation in pure form, crystallization, and characterization by single-crystal x-ray crystallography (Fig. 2B). Although P=P double bonds, such as that of the *bis*-$Cr(CO)_5$ complex of diphosphene PhP=PPh (*23*), can react with a diene to form a Diels-Alder adduct, double diene addition to two π bonds of a P_2 unit has not been reported. We propose that this reaction occurs in two steps: (i) transfer of P_2 to the first 1,3-CHD

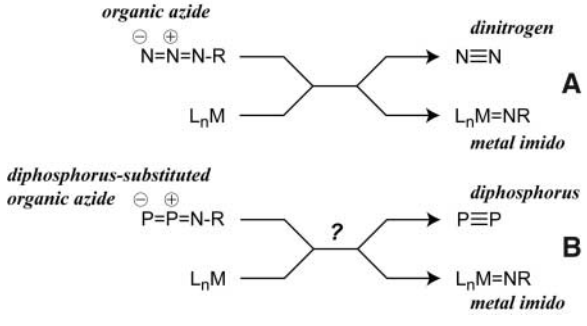

Fig. 1. (**A**) Reaction of an organic azide with a metal complex to extrude dinitrogen while delivering a metal imido unit and (**B**) the envisioned analogous process with diphosphorus extrusion.

Department of Chemistry, Massachusetts Institute of Technology, 77 Massachusetts Avenue, Cambridge, MA 02139–4307, USA.

*To whom correspondence should be addressed. E-mail: ccummins@mit.edu

molecule generating unobserved intermediate 2,3-diphosphabicyclo[2.2.2]octa-2,5-diene, depicted in brackets in Fig. 2A, and (ii) [4+2] cycloaddition of this intermediate to the second molecule of 1,3-CHD with endo stereoselectivity (selectivity such that the resulting C-C double bonds are proximal) (*22*, *24*). The tetracyclic structure of **3** with its cofacial pair of C=C π bonds is analogous to that of oligocondensed bicyclo[2.2.2]octenes studied as examples of laticyclic conjugation (*25*).

The use of excess 1,3-CHD is not required for thermal extrusion of P_2 from complex **1**. For example, at 50°C in toluene-d_8 solution, **1** was observed by ^{1}H NMR spectroscopy to decay to **2** with first-order rate constant $k = 4 \times 10^{-4}$ s^{-1}, with the appearance of imido **2** following the same kinetic profile. Under these conditions, however, no prominent signals were generated in the ^{31}P NMR spectrum of the reaction mixture, and the fate of the P_2 unit is not known. Also, pure **2** was obtained as golden yellow single crystals in 48% isolated yield following thermolysis of **1** in tetrahydrofuran (THF) solvent at 70°C for 45 min, and was characterized by x-ray diffraction (Fig. 2A). Notably, P_2 condensation is known to give the red modification of phosphorus, not the white phosphorus that is soluble and if formed would have been observed by ^{31}P NMR spectroscopy (*1*, *26*). Dimerization of two P_2 molecules to give P_4 is a process forbidden by orbital symmetry (*3*) and accordingly does not take place under mild conditions (*1*, *26*).

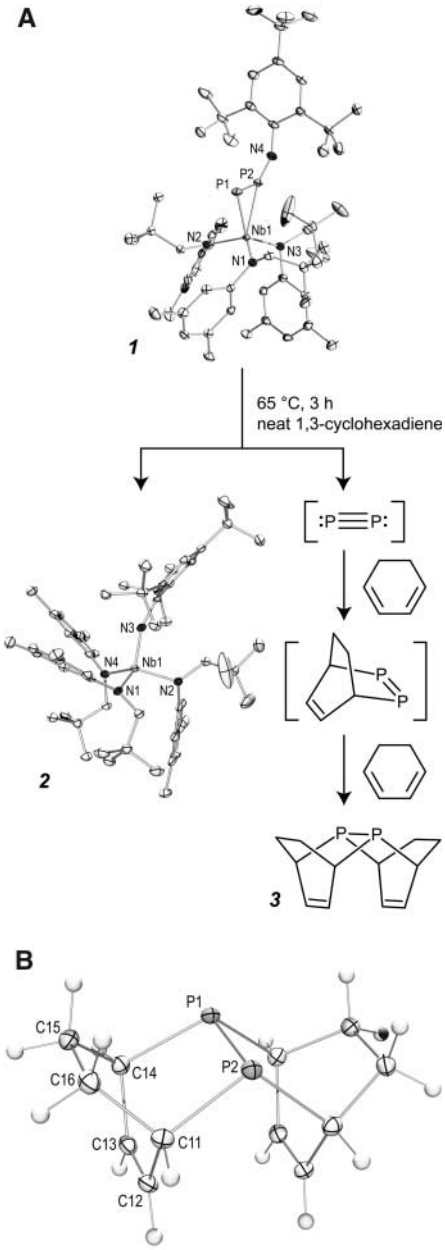

Fig. 2. (**A**) Heating a 1,3-CHD solution of niobium complex **1** results in P_2 extrusion and transfer into organodiphosphorus compound **3**. Thermal ellipsoid representations of **1** and **2** derived from x-ray diffraction studies are included. (**B**) Thermal ellipsoid rendering of organodiphosphorus compound **3**.

The combined observations are consistent with fragmentation of **1** to give **2** along with transient P_2 that subsequently can be trapped, as with 1,3-CHD. It is likely that **1** undergoes rearrangement from its solid-state structure **1**i (Fig. 3) to an alternative structure **1**ii or **1**iii, in which a Nb-N bond is formed, before loss of P_2. The proposed **1** → [**1**ii or **1**iii] → **2** + P_2 fragmentation is the simplest scenario consistent with all the available data and finds a close analogy in our recent description of C≡P triple-bond generation by unimolecular fragmentation of a niobium precursor (*27*) that has a metallacycle structure as in **1**ii.

Four possible isomeric forms of **1** (Fig. 3 and Table 1) have been investigated with the use of quantum chemical calculations. The lowest energy structure **1**i corresponds to the observed solid-state structure of **1** (Fig. 2A) and, on the basis of ^{31}P NMR shielding calculations, we also assign **1**i to be the structure adopted by **1** in solution. The next highest in energy is structure **1**iv, in which the PPNMes* ligand coordinates to niobium only through its terminal phosphorus atom; this structure is analogous to that of known tantalum and vanadium organic azide complexes (*15*–*17*). In addition, rearrangement of **1**i to **1**ii might be expected to take place through a structure such as **1**iv. The highest energy isomer is **1**iii, in which the PPNMes* ligand has migrated to an η^2-PN bonding mode and incorporates a one-coordinate phosphorus atom. Considering the energies of the computationally modeled isomers, a pathway passing through **1**ii as opposed to **1**iii is preferred. However, coordination of a Lewis acidic metal fragment, such as $W(CO)_5$, to the one-coordinate phosphorus atom of **1**iii might cause a pathway involving this isomer to become preferred. Notably, the computational study predicts, regardless of the microscopic pathway, that the fragmentation of **1** to **2** and P_2 is overall essentially thermoneutral.

In an effort to stabilize P_2 in solution after its extrusion from the $Nb(N[Np]Ar)_3$ platform, we investigated the possibility of its generation as a tungsten pentacarbonyl complex. Diphosphorus is already established as a ligand in transition-element chemistry, but as a rule it is found connected to two or more metal centers

Table 1. Model study of possible isomers of **1** and P_2 elimination. Calculations were performed at the BP86/TZ2P level of DFT theory using density functional theory methods. Ar^1 = 2,6-*t*-$Bu_2C_6H_3$, Me = CH_3, and Ph = C_6H_5. *E*(rel), the energy of **1**i to **1**iv relative to isomer **1**i. Δ*E*, the energy change for the fragmentation reaction of **1**i.

Model isomer or reaction	Complex	*E*(rel) or Δ*E* (kcal/mol)
(η^2-*PP*-Ar^{1}NPP)Nb(N[Me]Ph)$_3$	**1**i	0
(κ^2-*PN*-Ar^{1}NPP)Nb(N[Me]Ph)$_3$	**1**ii	+19
(η^2-*PN*-Ar^{1}NPP)Nb(N[Me]Ph)$_3$	**1**iii	+28
(η^1-*P*-Ar^{1}NPP)Nb(N[Me]Ph)$_3$	**1**iv	+6
1i→ (Ar^{1}N)Nb(N[Me]Ph)$_3$ + P_2		0

Fig. 3. Line drawings of four isomeric forms of **1** investigated using quantum chemical calculations. For simplicity, only a single resonance structure is drawn for each isomer.

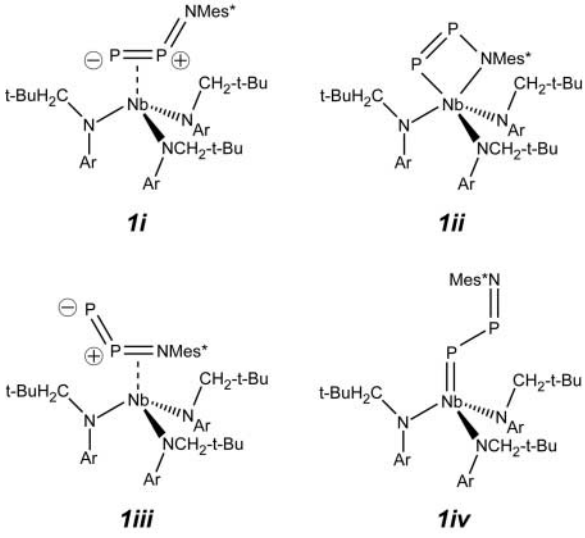

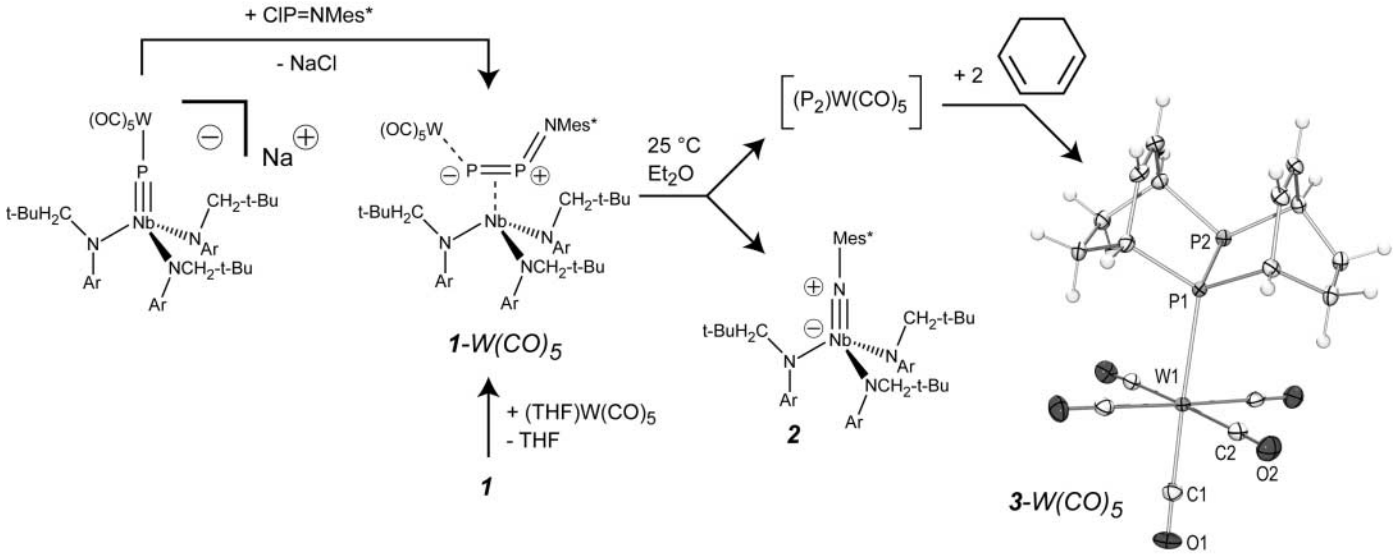

Fig. 4. Generation and trapping of a tungsten pentacarbonyl P_2 complex.

(*28*). Transition metal complexes of P_2 often are obtained as a result of P_4 activation (*29*), and white phosphorus is also known to serve as a P_2 source in organic reactions (*30*). We hoped that by binding P_2 to a single $W(CO)_5$ fragment, we would stabilize it sufficiently to extend its lifetime in solution but still retain triple-bond reactivity for the diphosphorus moiety. The targeted reactive intermediate—in this case, $(P_2)W(CO)_5$—has been the subject of a theoretical study concluding that, in contrast to N_2, the P_2 ligand preferentially binds side-on to the tungsten center (*31*).

The tungsten pentacarbonyl-capped phosphide anion $[(OC)_5W\text{-}P{\equiv}Nb(N[Np]Ar)_3]^{1-}$ was prepared by reaction of $W(CO)_6$ with phosphide anion $[P{\equiv}Nb(N[Np]Ar)_3]^{1-}$ and reacts with ClP=NMes* by means of salt elimination to generate **1**-$W(CO)_5$ (Fig. 4). The structure of this thermally unstable complex was confirmed spectroscopically. A pair of doublets at δ = 285 and 247 ppm with $^1J_{PP}$ = 730 Hz appear in the ^{31}P NMR spectrum of a benzene-d_6 solution at 20°C. Such a large coupling constant indicates the presence of substantial P-P multiple bonding in **1**-$W(CO)_5$. An alternative method for generation of **1**-$W(CO)_5$ exhibiting identical ^{1}H and ^{31}P NMR spectral properties was to add photochemically generated $(THF)W(CO)_5$ to a solution of **1** with liberation of THF (Fig. 4). The former method is preferred synthetically due to the relative ease of stoichiometry control.

At 10°C in toluene-d_8 solution, **1**-$W(CO)_5$ is seen to decay following clean first-order kinetics with a rate constant $k \approx 1.9 \times 10^{-4}$ s^{-1} in the presence of 0 to 80 equivalents of 1,3-CHD, as followed by ^{1}H NMR spectroscopy. The decay of **1**-$W(CO)_5$ under these conditions produces imido **2** together with the $W(CO)_5$ adduct of **3**. The insensitivity of the rate of this process to 1,3-CHD concentration strongly suggests that the rate-determining step is fragmentation to **2** and $(P_2)W(CO)_5$; subsequent sequential trapping of the latter by first one and then a second equivalent of 1,3-CHD (sequence not shown explicitly in Fig. 4) accounts for formation of **3**-$W(CO)_5$ (*32*). Diagnostic of **3**-$W(CO)_5$ are a pair of ^{31}P NMR doublets at $\delta = -34$ and -84 ppm with $^1J_{PP}$ = 340 Hz. The resonance at $\delta = -34$ ppm is assigned to the coordinated phosphorus in view of the flanking ^{183}W satellites it exhibits ($^1J_{WP}$ = 230 Hz). Confirming the formulation of **3**-$W(CO)_5$, identical spectral features were generated upon addition of (pyridine)$W(CO)_5$ to a sample of **3**. Additionally, **3**-$W(CO)_5$ was separated from **2**, and crystals grown from ether were subjected to a single-crystal x-ray diffraction study (Fig. 4).

The $W(CO)_5$-supported variant of the P_2 generation/transfer scheme is attractive for several reasons. The organic diene trap, 1,3-CHD, need not be used in excess for efficient interception of the putative $(P_2)W(CO)_5$ intermediate, and the fragmentation of **1**-$W(CO)_5$ takes place under ambient conditions without the need for heating. These features bode well for the extension of effective P_2 triple-bond reactivity to a wide substrate array, especially given the status of 1,3-CHD as a relatively unreactive Diels-Alder diene (*33*). As initial evidence that the trapping chemistry is not limited to 1,3-CHD as the organic partner, we found that both cyclopentadiene and 2,3-dimethylbutadiene serve as efficient traps for $(P_2)W(CO)_5$ with production, respectively, of corresponding tetra- and bicyclic organodiphosphorus compounds (*34*, *35*). Besides raising fundamental questions about the mechanism and scope of P_2 solution chemistry, the experimental observation of diphosphorus transfer into organic molecules creates the opportunity to test diphosphine structures such as **3** for utility as synthetic catalysts (*36*–*38*).

References and Notes

1. N. N. Greenwood, A. Earnshaw, *Chemistry of the Elements* (Butterworth-Heinemann, Boston, ed. 2, 1997).
2. D. P. Stevenson, D. M. Yost, *J. Chem. Phys.* **9**, 403 (1941).
3. H. Bock, H. Muller, *Inorg. Chem.* **23**, 4365 (1984).
4. O. J. Scherer, *Angew. Chem. Int. Ed. Engl.* **39**, 1029 (2000).
5. M. Regitz, O. J. Scherer, *Multiple Bonds and Low Coordination in Phosphorus Chemistry* (Thieme, Stuttgart, Germany, 1990).
6. K. B. Dillon, F. Mathey, J. F. Nixon, *Phosphorus: The Carbon Copy* (Wiley, Chichester, UK, 1998).
7. K. P. Huber, G. Herzberg, *Constants of Diatomic Molecules*, vol. IV of *Molecular Spectra and Molecular Structure* (Van Nostrand Reinhold, New York, 1979).
8. L. G. M. Pettersson, B. J. Persson, *Chem. Phys.* **170**, 149 (1993).
9. A. J. Sauval, J. B. Tatum, *Astrophys. J. Suppl. Ser.* **56**, 193 (1984).
10. N. Kobayashi, Y. Kobayashi, *Jpn. J. Appl. Phys.* **30**, L1699 (1991).
11. A. Kornath, A. Kaufmann, M. Torheyden, *J. Chem. Phys.* **116**, 3323 (2002).
12. M. McCluskey, L. Andrews, *J. Phys. Chem.* **95**, 2988 (1991).
13. L. Andrews, M. McCluskey, Z. Mielke, R. Withnall, *J. Mol. Struct.* **222**, 95 (1990).
14. Z. Mielke, M. McCluskey, L. Andrews, *Chem. Phys. Lett.* **165**, 146 (1990).
15. G. Proulx, R. G. Bergman, *J. Am. Chem. Soc.* **117**, 6382 (1995).
16. G. Proulx, R. G. Bergman, *Organometallics* **15**, 684 (1996).
17. M. G. Fickes, W. M. Davis, C. C. Cummins, *J. Am. Chem. Soc.* **117**, 6384 (1995).
18. J. S. Figueroa, C. C. Cummins, *Dalton Trans.* **2006**, 2161 (2006).
19. C. C. Cummins, *Angew. Chem. Int. Ed. Engl.* **45**, 862 (2006).
20. E. Niecke, J. Hombeuel, M. Blättner, V. Von Der Gönna, A. Ruban, in *Phosphorus, Arsenic, Antimony, and Bismuth*, H. H. Karsch, Ed., vol. 3 of *Synthetic Methods of Organometallic and Inorganic Chemistry*, W. A. Herrman, Ed. (Verlag, New York, 1996), pp. 28–30.

21. J. S. Figueroa, C. C. Cummins, *Angew. Chem. Int. Ed. Engl.* **43**, 984 (2004).
22. J. G. Martin, R. K. Hill, *Chem. Rev.* **61**, 537 (1961).
23. J. Borm, G. Huttner, O. Orama, L. Zsolnai, *J. Organomet. Chem.* **282**, 53 (1985).
24. R. Hoffmann, R. B. Woodward, *J. Am. Chem. Soc.* **87**, 4388 (1965).
25. W. Grimme *et al.*, *J. Chem. Soc., Perkin Trans. 2* 1893 (1998).
26. H. W. Melville, S. C. Gray, *Trans. Faraday Soc.* **32**, 271 (1936).
27. J. S. Figueroa, C. C. Cummins, *J. Am. Chem. Soc.* **126**, 13916 (2004).
28. O. J. Scherer, M. Ehses, G. Wolmershauser, *Angew. Chem. Int. Ed. Engl.* **37**, 507 (1998).
29. M. Ehses, A. Romerosa, M. Peruzzini, *Top. Curr. Chem.* **220**, 107 (2002).
30. C. Charrier, N. Maigrot, L. Ricard, P. LeFloch, F. Mathey, *Angew. Chem. Int. Ed. Engl.* **35**, 2133 (1996).
31. C. Esterhuysen, G. Frenking, *Chem. Eur. J.* **9**, 3518 (2003).
32. In the absence of 1,3-CHD, the rate constant for **1**-W(CO)$_5$ fragmentation is unchanged but the fate of (P_2)W(CO)$_5$ has not yet been determined.
33. J. Sauer, R. Sustmann, *Angew. Chem. Int. Ed. Engl.* **19**, 779 (1980).
34. Characterization data for the cyclopentadiene and 2,3-dimethylbutadiene reaction products are provided in the supporting online material text and figs. S7 and S8. For information on a structurally related diphosphorus bicycle synthesized by an unrelated method, see (*35*).
35. N. H. T. Huy, L. Ricard, F. Mathey, *J. Organomet. Chem.* **582**, 53 (1999).
36. X. F. Zhu, J. Lan, O. Kwon, *J. Am. Chem. Soc.* **125**, 4716 (2003).
37. J. E. Wilson, G. C. Fu, *Angew. Chem. Int. Ed. Engl.* **45**, 1426 (2006).
38. Experimental and computational details as well as x-ray diffraction data for **1**, **2**, **3**, and **3**-W(CO)$_5$ are provided as supporting material on *Science* Online.

39. We thank NSF for support of this research through grant CHE-0316823 and through a predoctoral fellowship to N.A.P. Complete crystallographic data were deposited in the Cambridge Crystallographic Database Centre (606636 to 606639).

Supporting Online Material

www.sciencemag.org/cgi/content/full/313/5791/1276/DC1
SOM Text
Figs. S1 to S13
Tables S1 to S3
References

8 May 2006; accepted 28 July 2006
10.1126/science.1129630

Discovery of a Young Planetary-Mass Binary

Ray Jayawardhana[1]* and Valentin D. Ivanov[2]

We have identified a companion to the young planetary-mass brown dwarf Oph 162225-240515. This pair forms a resolved binary consisting of two objects with masses comparable to those of extrasolar giant planets. Several lines of evidence confirm the coevality and youth of the two objects, suggesting that they form a physical binary. Models yield masses of ~14 and ~7 times the mass of Jupiter for the primary and the secondary object, respectively, at an age of ~1 million years. A wide (~240–astronomical unit) binary in the ultra-low-mass regime poses a challenge to some popular models of brown dwarf formation.

Brown dwarfs occupy the mass gap between dwarf stars and giant planets. Unlike stars, they are unable to fuse hydrogen because they have masses below the hydrogen-burning limit of ≈0.075 solar masses [≈75 times the mass of Jupiter ($M_{Jupiter}$)]. The distinction between brown dwarfs and planets is less clear. Some researchers draw the line at ≈13 $M_{Jupiter}$, because objects above that boundary can ignite deuterium, a less abundant isotope of hydrogen, for a short time early in their life, whereas those below ≈13 $M_{Jupiter}$ cannot. The vast majority of the hundreds of brown dwarfs identified since 1995 are free-floating objects, but a handful are in orbit around stars, further blurring the distinction between brown dwarfs and planets. Brown dwarfs and planets are often lumped together as substellar objects (*1*).

Among the most intriguing substellar objects identified to date are those with masses comparable to extrasolar giant planets (*2*, *3*). Unlike planets, these "planetary mass objects" ("planemos" for short), or "sub–brown dwarfs," as they are sometimes called, are not bound to stars. Because planemos represent the lowest mass free-floating objects known, determining whether they form the same way as stars and higher mass brown dwarfs will advance our understanding of the star-formation process. Some planemos appear to harbor accretion disks (*4*, *5*), just like stars and brown dwarfs at young ages (*6*–*8*). The existence of disks around all three classes of objects suggests that they have a common origin. Binary properties of planemos could provide a more definitive test, because some formation models predict a low binary frequency and a paucity of wide pairs at the lowest masses (*9*, *10*). Here, we report the identification of a wide binary system consisting of two planemos.

An optical *I*-band image of the young planetary-mass brown dwarf Oph 162225-240515 (hereafter Oph 1622-2405) (*5*, *11*, *12*), taken with the European Southern Observatory's (ESO's) New Technology Telescope using the ESO Multimode Instrument (EMMI), showed a candidate companion at a separation of ≤2″. Therefore, we obtained optical spectra of both objects with the Focal Reducer/low-dispersion Spectrograph-2 (FORS2) and near-infrared J_s-, H-, K_s-, and L'-band images with the Infrared Spectrometer and Array Camera (ISAAC) on ESO's Very Large Telescope UT2, under excellent seeing conditions (*13*).

The binary is well resolved in all of our imaging and spectroscopic data. It has a separation of 1.94″ ± 0.01″ (±SD) and a position angle of 182.2° ± 0.4° (table S1). At a distance of 125 pc (*11*), this corresponds to a projected separation of ≈242 astronomical units (AU). The colors of the secondary are slightly more red than those of the primary (Fig. 1), consistent with its being a somewhat cooler object. We measured a brightness difference of 1.4 ± 0.1 magnitudes (mag) between the two objects in the optical *I* band (*13*). In the near-infrared, we found J_s = 14.65 ± 0.05 (mag), H = 14.19 ± 0.05 (mag), K_s = 13.66 ± 0.06 (mag), and L' = 13.23 ± 0.05 (mag) for the primary, and J_s = 15.41 ± 0.05 (mag), H = 14.87 ± 0.05 (mag), K_s = 14.22 ± 0.06 (mag), and L' = 13.61 ± 0.06 (mag) for the secondary.

By examining a variety of features (e.g., TiO and VO absorption troughs) as well as the overall shapes of the spectra in comparison to those of cool field dwarfs (*14*), we derived best-match spectral types of M9 for the primary and M9.5-L0 for the secondary (Fig. 2) (*5*). These spectral types imply effective temperatures of 2400 and 2100 K, respectively (*15*), with an uncertainty of ±100 K. The infrared colors of the two components of the binary are also consistent with their having spectral types in the late M–early L range (*16*). Furthermore, the

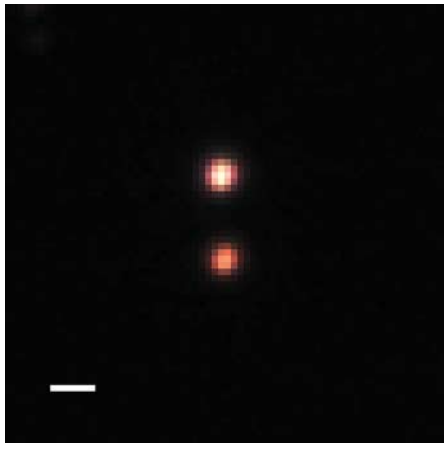

Fig. 1. A three-color J_s-H-K_s image of Oph 162225-240515AB. North is up, and East is to the left. The field of view is 10″ × 10″, and the scale bar indicates 1″. The apparent separation of the binary is 1.94″, corresponding to 242 AU at a distance of 125 pc.

[1]Department of Astronomy and Astrophysics, University of Toronto, Toronto, ON M5S 3H8, Canada. [2]European Southern Observatory, Avenida Alonso de Cordova 3107, Vitacura, Santiago 19001, Chile.

*To whom correspondence should be addressed. E-mail: rayjay@astro.utoronto.ca